Asian Journal of Chemistry; Vol. 29, No. 6 (2017), 1270-1274

ASIAN JOURNAL OF CHEMISTRY

https://doi.org/10.14233/ajchem.2017.20461

Synthesis and Characterization of $Ca_{1-x}Co_xTiO_3$ and its Photocatalytic Activity on Photodegradation of Methylene Blue

A.K. PRODJOSANTOSO[1,*], C. KUSUMAWARDANI[1], M.P. UTOMO[1] and C.T. HANDOKO[2]

[1]Chemistry Department, Yogyakarta State University, Yogyakarta 5528, Indonesia
[2]Environmental Science Department, University of Sriwijaya, Palembang 30662, Indonesia

*Corresponding author: E-mail: prodjosantoso@uny.ac.id

Received: 21 December 2016; *Accepted*: 18 February 2017; *Published online*: 10 April 2017; AJC-18338

A series of $Ca_{1-x}Co_xTiO_3$ has been prepared through the ceramic method as polycrystalline powders with x = 0, 0.01, 0.025, 0.05 and 0.1. The structure of resulting materials was refined from a powder X-ray diffraction using the Rietvield method showing the perovskite-type structure isostructural with $CaTiO_3$. The morphology and particle size of $Ca_{1-x}Co_xTiO_3$ were studied using SEM/EDX that showed a particle size of around 3.5 nm with non-homogenous particle sphere shapes. The electronic structure of $Ca_xCo_{1-x}TiO_3$ was studied by UV/visible spectroscopy method, which showed that the prepared $Ca_{1-x}Co_xTiO_3$ having good response in the visible region with the band gap energy (E_g) of around 2.2 eV, which is highly potent as visible light photocatalysts. The adsorption capacity and adsorption equilibrium constant of the oxides to the methylene blue were also studied. The adsorption process in $Ca_{1-x}Co_xTiO_3$ materials follows the Langmuir adsorption type as a consequence of homogenous pore structures. The catalytic activity of $Ca_{1-x}Co_xTiO_3$ on the methylene blue degradation are also discussed.

Keywords: $Ca_{1-x}Co_xTiO_3$, Perovskite structure, Visible-light photocatalyst.

INTRODUCTION

The perovskite structure compound, ABO_3 and its derivatives are widely investigated due to their significance in both fundamental research and the high potential applications because of their diverse physical properties [1-3]. The $MTiO_3$ perovskite (where M = Ca, Sr or Ba) is one of the most attracting materials since it has a unique electronic structure and so it is developed for solar applications, such as photoelectrochemical cells, solar cells and photovoltaic technologies [4]. The compounds are modified by replacing small amount of M^{2+} with other cations to enhance the photoactivity of the perovskites [5,6].

Perovskite materials have been synthesized by serial methods, such as hydrothermal, sol gel, but mostly by solid state reaction to produce polycrystalline samples [7-10]. The starting materials are usually simple binary oxides or salts reacted at a relatively high temperatures [11,12]. Here, we report a simple ceramic method to synthesize $Ca_{1-x}Co_xTiO_3$ perovskite from $CaCO_3$ and $CoCO_3$ precursors with variation of x between 0 to 0.1. The prepared materials are then applied as photocatalyst materials in the methylene blue degradation [12-14]. The contribution of cobalt content in $Ca_{1-x}Co_xTiO_3$ materials to the increase of the maximum adsorption capacity, the adsorption equilibrium constant and the kinetic constant of methylene blue photocatalytic oxidation in aqueous suspension were investigated simultaneously.

EXPERIMENTAL

$CaCO_3$ (Merck), $Co(NO_3)\cdot 6H_2O$ (Merck), TiO_2 (Merck) and methylene blue (Sigma-Aldrich) were used as received without any further purification.

The $Ca_{1-x}Co_xTiO_{3-}$ was synthesized by calcining the stoichiometric mixture of $CaCO_3$, $Co(NO_3)\cdot 6H_2O$ and TiO_2 in a muffle furnace at 700, 800, 900 and 1100 °C for 12 h every step with grinding treatment in between calcination processes. The resulting materials were then characterized using powder X-ray diffraction (XRD Rigaku Multiflex), scanning electron microscopy (SEM Jeol JCM-6000), porosimetry and UV-visible spectroscopy (UV-2450PC Pharmaspec spectrophotometer) methods.

The adsorption behaviour of $Ca_{1-x}Co_xTiO_{3-}$ were determined as follow: a set of adsorption test was performed in the dark, in which 10 mL of methylene blue solutions with different initial concentrations were added with 0.1 g of $Ca_{1-x}Co_xTiO_3$ powders and then put into a shaker for 24 h. The methylene blue concentration in the suspensions before and after the

adsorption were analyzed to determine the amount of methylene blue adsorbed by the catalyst.

The photocatalytic activity of $Ca_{1-x}Co_xTiO_{3-}$ was determined by measuring the decomposition of methylene blue under visible and UV-light. The initial concentration of methylene blue was 1×10^{-5} M. The methylene blue taken at given time intervals was centrifuged and then determined with a spectrophotometer by measuring the absorbance at 663.5 nm, respectively. For comparison, a photocatlytic activity reaction was also carried out using commercial titania powder (Degussa P-25).

RESULTS AND DISCUSSION

The crystalline compound of $Ca_{1-x}Co_xTiO_3$ (x = 0, 0.025. 0.05 and 0.1) have been succesfully synthesized through a ceramic method. The XRD patterns of the compounds are similar indicating that the samples are isostructural (Fig. 1). The peaks fit well with those assigned in JCPDS card No. 86-1393. The lines shifting were caused by the varied amount of Co in $CaTiO_3$ lattice. The Rietica program [15] was used to study the structure of $Ca_{1-x}Co_xTiO_{3-}$ based on powder XRD data. The result showed that $Ca_{1-x}Co_xTiO_{3-}$ materials are orthorombic crystal type with P_{bnm} group space. Lattice parameter, crystal volume, atomic distance, atomic position, valence bond and coordination number of $Ca_{1-x}Co_xTiO_3$ are presented in Tables 1-4, respectively. The lattice parameters decrease along with the decreasing amount of Ca in the compound. This is as a consequence of the smaller Co atomic size compare to Ca, in which Co is positioned in Ca sites. The valence proportion of Ca/Co to Ti is approximately 1:2, means that it qualifies the compound neutrality law.

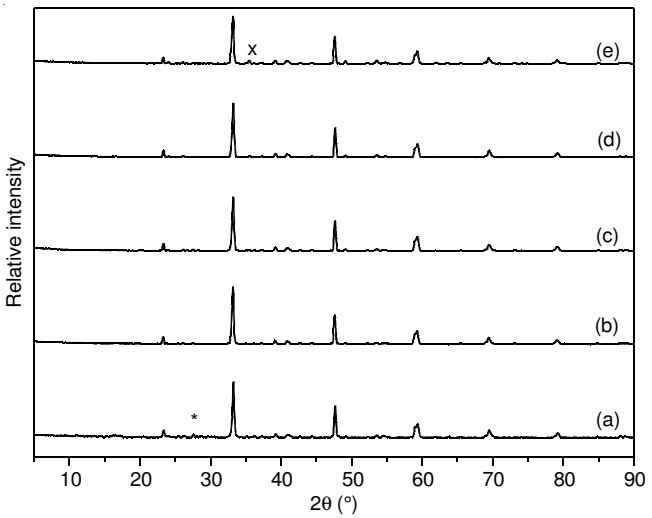

Fig. 1. Powder XRD pattern of $Ca_{1-x}Co_xTiO_{3-}$, x = 0 (a); x=0.001 (b); x = 0.025 (c); x = 0.05 (d) and x = 0.1 (e). A weak line at $2\theta = 27{,}56^0$ (*) indicates TiO_2 rutile phase and $2\theta = 35{,}44^0$ (x) $CoTiO_3$

The SEM method was employed to study the shape and morphology of $Ca_{1-x}Co_xTiO_3$. Fig. 2 indicates $Ca_{1-x}Co_xTiO_{3-}$ (x = 0.001), typical of the samples. All materials are having non-

TABLE-1
LATTICE PARAMETER OF $Ca_{1-x}Co_xTiO_3$

$Ca_{1-x}Co_xTiO_3$	Lattice parameter (Å)			Crystal volume (Å^3)	R_p	R_{wp}	R_{exp}	GOF	R_{Bragg}
	a	b	c						
x = 0	5.4018(6)	5.4516(6)	7.6650(9)	225.72(4)	14.01	19.93	33.76	0.35	4.36
x = 0.001	5.4016(3)	5.4511(3)	7.6648(5)	225.69(2)	10.74	14.73	17.95	0.67	5.53
x = 0.025	5.4003(4)	5.4518(4)	7.6644(6)	225.65(3)	10.70	15.74	17.78	0.78	5.42
x = 0.050	5.3985(3)	5.4519(3)	7.6643(5)	225.58(3)	10.76	16.31	17.87	0.83	5.85
x = 0.100	5.3966(6)	5.4504(5)	7.6591(7)	225.30(3)	11.15	15.82	18.25	0.75	4.69

TABLE-2
ATOMIC DISTANCES OF $Ca_{1-x}Co_xTiO_3$

Atomic distances	x = 0	x = 0.001	x = 0.025	x = 0.05	x = 0.1
Ca/Co-O1	2.3344(3)	2.3573(1)	2.3354(2)	2.3227(1)	2.3291(2)
Ca/Co-O2	2.4510(2)	2.3698(1)	2.3822(2)	2.3998(1)	2.3911(2)
Ti-O1	1.9656(2)	1.9602(1)	1.9634(2)	1.9669(1)	1.9649(2)
Ti-O2	1.9246(2)	1.9554(1)	1.9609(1)	1.9513(1)	1.9468(2)

TABLE-3
ATOMIC POSITIONS OF $Ca_{1-x}Co_xTiO_3$

Atoms	x = 0			x = 0.001			x = 0.025		
	x	y	z	x	y	z	x	y	z
Ca/Co	0.9884(13)	0.0310(7)	0.2500(0)	0.9913(7)	0.0332(3)	0.2500(0)	0.9916(8)	0.0336(4)	0.2500(0)
Ti	0.0000(0)	0.5000(0)	0.0000(0)	0.0000(0)	0.5000(0)	0.0000(0)	0.0000(0)	0.5000(0)	0.0000(0)
O1	0.0809(21)	0.4959(21)	0.2500(0)	0.0750(11)	0.4853(9)	0.2500(0)	0.0784(12)	0.4879(10)	0.2500(0)
O2	0.7110(16)	0.2825(18)	0.0236(14)	0.7075(9)	0.2895(10)	0.0357(7)	0.7092(10)	0.2900(10)	0.0342(8)
Atoms	x = 0.05			x = 0.1					
	x	y	z	x	y	z			
Ca/Co	0.9920(8)	0.0313(5)	0.2500(0)	0.9900(9)	0.0350(5)	0.2500(0)			
Ti	0.0000(0)	0.5000(0)	0.0000(0)	0.0000(0)	0.5000(0)	0.0000(0)			
O1	0.0803(12)	0.4830(13)	0.2500(0)	0.0809(17)	0.4887(11)	0.2500(0)			
O2	0.7145(10)	0.2859(10)	0.0346(8)	0.7117(12)	0.2905(13)	0.0333(9)			

TABLE-4
BOND VALENCES (BV) AND COORDINATION NUMBERS (CN) OF $Ca_{1-x}Co_xTiO_3$

Bonds	x = 0			x = 0.001			x = 0.025			x = 0.05			x = 0.1		
	BV	Σ	CN	BV	Σ	CN	BV	Σ	CN	BV	Σ	CN	BV	Σ	CN
Ca/Co-O1	0.68	1.94	4	0.69	2.05	4	0.70	2.04	4	0.72	2.04	4	0.71	2.05	4
Ca/Co-O2	1.26		8	1.36		8	1.34		8	1.32		8	1.34		8
Ti-O1	1.35	4.03	2	1.35	4.03	2	1.34	4.04	2	1.33	4.07	2	1.33	4. 05	2
Ti-O2	2.68		4	2.68		4	2.70		4	2.74		4	2.72		4

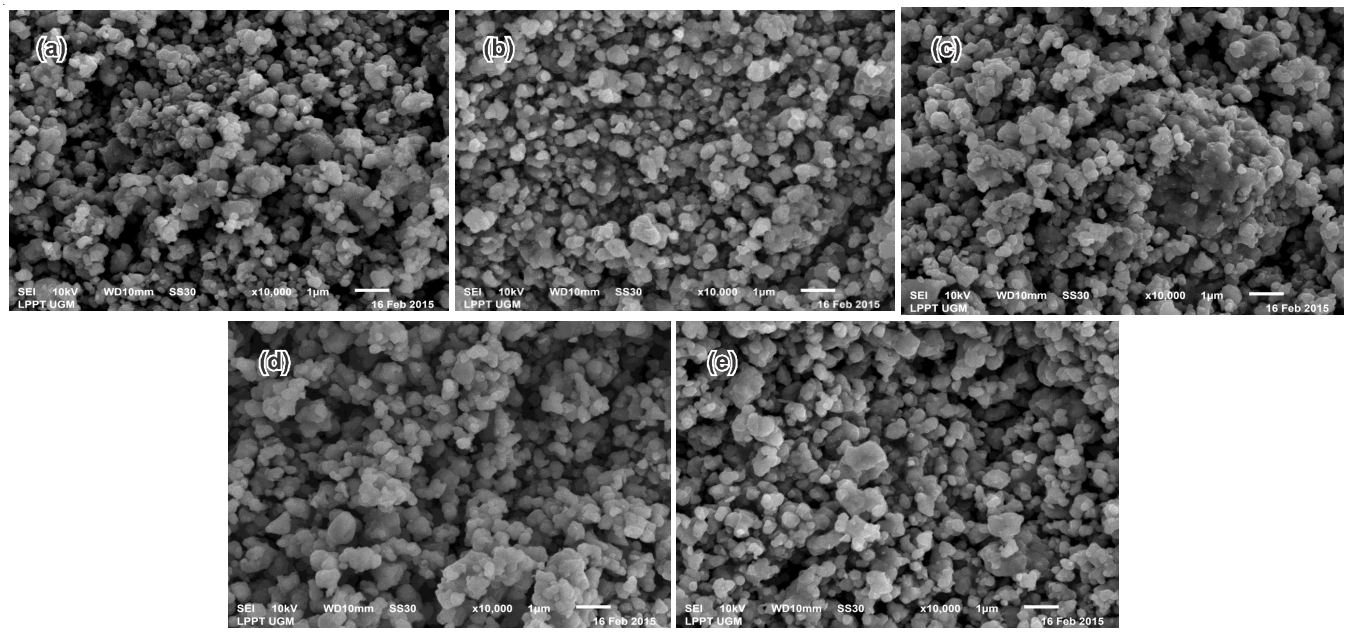

Fig. 2. SEM image of $Ca_{1-x}Co_xTiO_3$ with x = 0 (a); 0.001(b); 0.025 (c); 0.5 (d) and 0.1 (e)

uniform porous structure with particle size in the range of 0.5-1.5 μm. Electron dispersive X-ray (EDX) analysis confirmed that all samples are indicating the compound of $Ca_{1-x}Co_xTiO_3$ (x = 0, 0.001, 0.025, 0.05 and 0.1) with acceptable errors and are in agreement with the stoichiometric precursors used in the synthesis process.

The band gap energy (E_g) of $Ca_{1-x}Co_xTiO_3$ was determined based on UV/visible absorption spectra (Fig. 3), following Kubelka Munk formula. The obtained E_g are listed in Table-5. There is no specific trend in band gap energy values according to the different x composition, but the results indicated that the doped cobalts lead to the decrease of band gap energy both in direct and indirect band gap energies. The lower band gap energy means that the material is having higher activity in near visible region.

To investigate the effects of Co doping on catalysts' surface area, BET test was carried out to determine the surface area as listed in Table-6. It can be seen that the x value significantly

TABLE-5
BAND GAP ENERGY OF $Ca_{1-x}Co_xTiO_3$

$Ca_{1-x}Co_xTiO_3$	Band gap energy (eV)	
	E_g indirect	E_g direct
x = 0	4.23	3.38
x = 0.001	3.79	3.12
x = 0.025	3.97	2.71
x = 0.050	3.91	2.68
x = 0.100	3.81	2.74

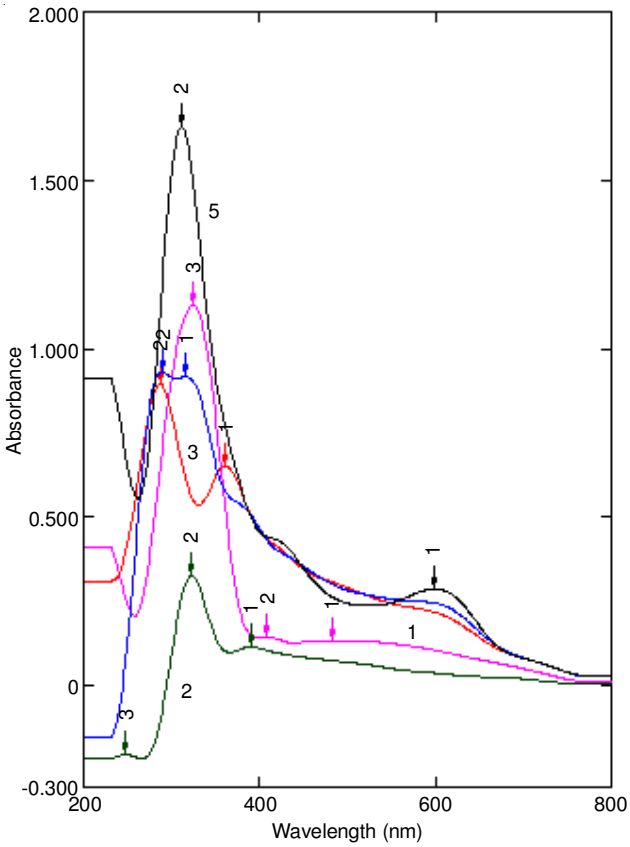

Fig. 3. UV/visible spectra of $Ca_{1-x}Co_xTiO_3$ with x = 0-0.1

TABLE-6
SURFACE AREA OF $Ca_{1-x}Co_xTiO_3$

$Ca_{1-x}Co_xTiO_3$	BET (m^2/g)
x = 0	3.9220
x = 0.001	4.4116
x = 0.025	8.2681
x = 0.050	2.9523
x = 0.100	5.4518

influences the catalyst's surface area and there is an optimum x that provided the highest surface area; with x = 0.025 resulted in surface area of 8.2681 m^2/g.

In order to investigate the influence of adsorption process on the photocatalysis reaction, adsorption tests were carried out in the dark to study the adsorption isotherm of methylene blue on the prepared catalyst. The adsorption data were then fitted to obtain the adsorption model of the catalyst to methylene blue (Fig. 4) which showed that all prepared catalyst showed the typical of Langmuir adsorption model. It also confirmed from C/G *versus* C plots as shown in Fig. 6, which were well fitted by the Langmuir adsorption model [16,17] as follows:

$$\frac{C}{\Gamma} = \frac{C}{\Gamma_{max}} + \frac{1}{K_a \Gamma_{max}}$$

where C is the equilibrium concentration of the substrate in the solution (mol/L), K_a is adsorption equilibrium constant (L mol^{-1}), Γ is adsorbed methylene blue per gram catalyst (mol g^{-1}) and Γ_{max} is saturated adsorption capacity (mol g^{-1}). The values of Γ_{max} and K_a were obtained from the above plot fitting and listed in Table-7. The result indicated that relation between structural properties to the adsorption equilibrium constant (Ka). It seems that the change of physical properties of the catalyst owing to cobalt doping, such as specific surface area, porosity and total pore volume, have influenced the adsorption capacity of the catalyst. The catalyst which have higher specific surface area have a better adsorption capacity and adsorption constant.

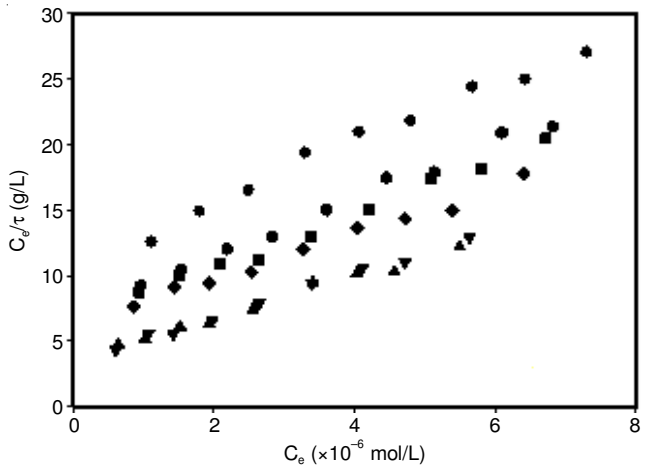

Fig. 4. UV/visible spectra of $Ca_{1-x}Co_xTiO_3$ with x = 0 - 0.1

Based on the adsorption capacity data, we have chosen a material with lowest adsorption capacity to perform the photocatalytic test, *i.e.* $Ca_{0.975}Co_{0.25}TiO_3$. The photocatalytic activity of prepared catalyst samples have been studied by measuring the percentage decomposition of methylene blue

TABLE-7
ADSORPTION ISOTHERM DATA OF PREPARED $Ca_{1-x}Co_xTiO_3$ CATALYST IN METHYLENE BLUE SYSTEM

$Ca_{1-x}Co_xTiO_3$	Saturated adsorption capacity (Γ_{max} 10^{-6} mol g^{-1})	Adsorption equilibrium constant (Ka, L mol^{-1})	R^2
Pure titania (Degussa P25)	4.39	20867.89	0.6833
x = 0	4.95	30832.51	0.7812
x = 0.001	6.42	37897.97	0.7653
x = 0.025	5.92	49860.05	0.8375
x = 0.050	5.73	28189.30	0.7923
x = 0.100	4.63	39968.35	0.8016

aqueous solution under visible and UV-light with initial concentration of 10^{-5} mol/L. The experimental result of the photocatalytic test was shown in Fig. 5, which demonstrated that the catalyst has a high activity both in UV and visible area. It also showed that the catalyst with higher saturated adsorption capacity and adsorption equilibrium constant were having better activity as methylene blue photodegradation catalyst. That is meant that the adsorption process has been an important part of the photocatalytic process in the catalyst. Therefore, the Langmuir-Hinshelwood (L-H) kinetic equation is being an appropriate model to describe this kind of reaction.

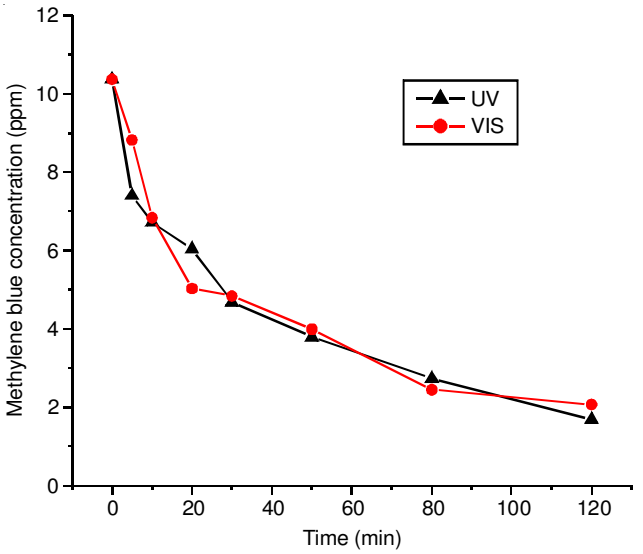

Fig. 5. Photoactivity of $Ca_{0.975}Co_{0.25}TiO_3$ on methylene blue photodegradation under UV and visible light

Langmuir-Hinshelwood kinetics is the most commonly used kinetic expression to explain the kinetics of heterogeneous catalytic process, which can be simplified into the first order model if the substrate concentration (C) is very low. The kinetics constant (k_1) of methylene blue photodegradation could be calculated by using the integrated of Langmuir-Hinshelwood (L-H) model [18] which is given by:

$$r = -\frac{dC}{dt} = \frac{kK_aC}{1 + K_aC}$$

The integrated expression of this equation given by:

$$\ln\left(\frac{C_o}{C}\right) + Ka(C_o - C) = kK_a t$$

where K_a is the adsorption equilibrium constant, which already determined from dark adsorption test. The k is the photo-reaction rate constant (min^{-1}), t is the reaction time (min) and C_o is initial concentration.

If the term $K_aC << 1$; r = kKaC and its integration to limits: C = Co at t = 0 and C = C_t at t = t lead Langmuir-Hinshelwood expression reduces to a first order kinetics and formulated as follow:

$$-\ln\frac{C}{C_o} = k_1 t$$

where k_1 is the apparent rate constant (min^{-1}) and $k_1 = kK_a$. The kinetic parameters (k_1 and k) were obtained from the fitting of ln (C/C_o) *vs*. t plot. The kinetics data showed that the synthesized catalyst demonstrated better performance in the methylene blue photodegradation than the pure TiO_2 (Degussa P25). The apparent rate constant, k_1, of the were more than three times higher compared to the pure TiO_2. Whereas the photo-reaction rate constant, k, of the synthesized catalyst were two times higher compared to the pure one in average. It was obviously that the visible-light activity of prepared $Ca_{1-x}Co_xTiO_3$ was better than that of pure titania.

Conclusion

$Ca_{1-x}Co_xTiO_{3-}$ photocatalysts have been prepared by ceramic route. The advantages of this method over other methods of preparation are (i) use of inexpensive chemical precursors and (ii) formation of uniformly sized nanoparticles. The $Ca_{1-x}Co_xTiO_{3-}$ had larger crystallite size with the increase of doped cobalt. Optical absorption studies clearly identified the visible light response with the existence of cobalt. A higher photocatalytic activity for the decomposition of methylene blue in the visible region has been obtained for the prepared $Ca_{1-x}Co_xTiO_{3-}$ sample compared to pure TiO_2.

ACKNOWLEDGEMENTS

Financial support from Indonesian Government through HIBAH BERSAING Grants contract No: 33/PSN-DIKTI/UN.34.21/2015 is gratefully acknowledged.

REFERENCES

1. R.E. Cohen, *Nature*, **358**, 136 (1992); https://doi.org/10.1038/358136a0.
2. Y. Hu, J. Schlipf, M. Wussler, M.L. Petrus, W. Jaegermann, T. Bein, P. Müller-Buschbaum and P. Docampo, *ACS Nano*, **10**, 5999 (2016); https://doi.org/10.1021/acsnano.6b01535.
3. P. Kanhere and Z. Chen, *Molecules*, **19**, 19995 (2014); https://doi.org/10.3390/molecules191219995.
4. J. Shi, W.J. Lee, Y. Liu, Y. Yang and P. Wang, *IEEE Trans. Ind. Appl.*, **48**, 1064 (2012); https://doi.org/10.1109/TIA.2012.2190816.
5. N. Pellet, P. Gao, G. Gregori, T.Y. Yang, M.K. Nazeeruddin, J. Maier and M. Grätzel, *Angew. Chem. Int. Ed.*, **53**, 3151 (2014); https://doi.org/10.1002/anie.201309361.
6. J.W. Shi and L.J. Guo, *Prog. Nat. Sci. Mater. Int*., **22**, 592 (2012); https://doi.org/10.1016/j.pnsc.2012.12.002.
7. J. Tian, L. Chen, J. Dai, X. Wang, Y. Yin and P. Wu, *Ceram. Int.*, **35**, 2261 (2009); https://doi.org/10.1016/j.ceramint.2008.12.010.
8. M. Cernea, F. Vasiliu, C. Plapcianu, C. Bartha, I. Mercioniu, I. Pasuk, R. Lowndes, R. Trusca, G.V. Aldica and L. Pintilie, *J. Eur. Ceram. Soc.*, **33**, 2483 (2013); https://doi.org/10.1016/j.jeurceramsoc.2013.03.026.
9. L. Chen, F. Tang, Y. Wang, S. Gao, W. Cao, J. Cai and L. Chen, *Nano Res.*, **8**, 263 (2015); https://doi.org/10.1007/s12274-014-0662-1.
10. S.A. Veldhuis, P.P. Boix, N. Yantara, M. Li, T.C. Sum, N. Mathews and S.G. Mhaisalkar, *Adv. Mater.*, **28**, 6804 (2016); https://doi.org/10.1002/adma.201600669.
11. M.W. Li, G. Xiao-Mei, H. Yin-Ling and W. Chen-Yang, *J. Nano Electron Phys.*, **5**, 1 (2013).
12. V. Sharad Gaikwad, B. Ashok and B.G. Vishwas, *Der Pharma Chemica*, **4**, 184 (2012).
13. S. Shahabuddin, N.M. Sarih, S. Mohamad and J.J. Ching, *Polymers*, **8**, 27 (2016); https://doi.org/10.3390/polym8020027.
14. A. Al-Kdasi, A. Idris, K. Saed and C.T. Guan, *Global Nest Int. J.*, **6**, 222 (2004).
15. B.A. Hunter, and C.J. Howard, A Computer Program for the Rietveld Analysis of X-ray and Neutron Powder Diffraction Patterns, (1996).
16. M.B. Desta, *J. Thermodyn.*, **2013**, 1 (2013); https://doi.org/10.1155/2013/375830.
17. A.W. Marczewski, *Langmuir*, **26**, 15229 (2010); https://doi.org/10.1021/la1010049.
18. J.P.S. Valente, P.M. Padilha and A.O. Florentino, *Chemosphere*, **64**, 1128 (2006); https://doi.org/10.1016/j.chemosphere.2005.11.050.